Available online at www.sciencedirect.com

SciVerse ScienceDirect

Ceramics International 39 (2013) 7743–7750

CERAMICS INTERNATIONAL

www.elsevier.com/locate/ceramint

Crystallization behavior and properties of K_2O–CaO–Al_2O_3–SiO_2 glass-ceramics

Jianfang Wu, Zhen Li*, Yanqiu Huang, Fei Li

Engineering Research Center of Nano-Geomaterials of Ministry of Education, Faculty of Materials Science and Chemistry, China University of Geosciences, Wuhan, 430074, PR China

Received 2 January 2013; received in revised form 8 March 2013; accepted 11 March 2013
Available online 18 March 2013

Abstract

In order to obtain high-strength anorthite glass-ceramics, K_2O–CaO–Al_2O_3–SiO_2 quaternary glass and relevant glass-ceramics were prepared and investigated. The results show that anorthite along with kalsilite or leucite was precipitated from the parent glass. Kalsilite crystals were formed firstly and then converted into leucite through reacting with SiO_2 in the glass phase. The morphology of the crystals was dependent on the heat-treatment temperature. Column crystals were transformed into fine granular grains when the sintering temperature changed from 900 °C to 1100 °C. The activation energy (E_α) and avrami constant (n) were also calculated as 463.81 KJ/mol and 3.74 respectively, indicating that bulk nucleation and three-dimensional crystal growth were the dominating mechanisms in the temperature range 1000–1100 °C. The maximum value of the flexural strength for the glass-ceramics containing leucite was 248 MPa and the coefficient of thermal expansion (CTE) was in the range $5.69 \sim 11.94 \times 10^{-6}\,K^{-1}$. The leucite is the main reason for the high CTEs and high flexural strength of glass-ceramics.

Keywords: C. Thermal expansion; Glass-ceramic; Anorthite; Crystallization behavior; Flexural strength

1. Introduction

Glass-ceramics are polycrystalline materials produced by melt quenching technique and subsequently converted into fine grained ceramics by appropriate heat-treatment [1,2], which exhibit advantageous thermal, optical, chemical, mechanical and electrical properties [3]. The great varieties of compositions and microstructures with specific technological properties have allowed glass-ceramics to be used in a wide range of applications. For the glass-ceramics, the two important effects that determine their properties are the crystalline phases and the microstructures [4], which all can be tailored by the chemical composition [5–7], heat-treatment [8] and even the employed nucleating agents [9]. When developing a new kind of glass-ceramic, it is vital to control the crystallization of the parent glass. Regarding the kinetic parameters, the activation energy of crystallization (E_α) and crystal growth index (Avrami constant: n) are the key parameters to judge the crystallization capability of the parent glass and describe the micro-morphology of the crystals, respectively. As the E_α is related to the certain energy barrier when glassy phases transform to crystalline phase(s), it will be easier for the glass to crystallize if the E_α is lower. And the n is a dimensionless constant related to the nucleation and growth mechanisms. Different micro-morphological crystals could be precipitated from the parent glass with different values of n [10–13]. Generally, one-dimensional needles or columns, two-dimensional plates and three-dimensional polyhedrons or particles would be precipitated from the parent glass when the calculated values of n are 2, 3 and 4.

Anorthite glass-ceramics obtained by crystallization of glass powder have attracted attention in many fields, such as substrate materials for low temperature co-fired ceramic application [14–18], package materials for lighting-emitting diode (LED) chips [19], dental materials [20], porcelain stoneware body materials [21], and so on, because of their high chemical durability, low dielectric constant and loss,

*Correspondence to: Faculty of Materials Science and Chemistry, China University of Geosciences, No. 388, Lumo Road, Wuhan 430074, PR China. Tel.: +86 27 18971473850.
E-mail addresses: zhenli@cug.edu.cn, jfw2011@sina.com (Z. Li).

0272-8842/$ - see front matter © 2013 Elsevier Ltd and Techna Group S.r.l. All rights reserved.
http://dx.doi.org/10.1016/j.ceramint.2013.03.031

applicable coefficient of thermal expansion and applicable strength.

Leucite ($KAlSi_2O_6$) is a framework pseudotetragonal aluminosilicate. Its structure consists of corner-linked (Al, Si)O_4 tetrahedra filled with K^+ cations [22]. It exhibits an interesting reversible phase transition in the temperature range 620–690 °C [23]. At room temperature the leucite has a tetragonal symmetry, but the crystal structure transforms to cubic structure at high temperature. The phase transformation of leucite from cubic to tetragonal will lead to a reversible 1.2% volume contraction. Together with the difference in thermal expansion between the tetragonal leucite crystals and the surrounding phases, high tangential compressive stresses around the leucite grains should be developed and maintained during the cooling process, which are considered responsible for strengthening in leucite glass-ceramics [24–26]. So leucite was widely introduced into feldspathic glass-ceramic materials as a reinforcing phase [27–30].

In this work, a brand-new kind of anorthite glass-ceramic containing leucite from K_2O–CaO–Al_2O_3–SiO_2 quaternary glass was investigated. The anorthite glass-ceramics exhibit extraordinary characteristics. Another advantage of this new glass-ceramic is the lower cost comparing to traditional glass-ceramics fabricated by chemical pure materials, because potassium feldspar was used as the main raw material, which is one of the most abundant minerals in the earth's crust. Hence, the glass-ceramic materials in this work deserve further research for their superiorities in many potential applications.

2. Experimental and methods

2.1. Glass preparation

A potassium feldspar from China, CaO (Analytical reagent, Shanghai Chemicals Co. Ltd.) and Al_2O_3 (Analytical reagent, Shanghai Chemicals Co. Ltd.) were used as raw materials to prepare K_2O–CaO–Al_2O_3–SiO_2 quaternary glass. The chemical compositions of the potassium feldspar and of the selected glass were summarized in Table 1. The molar ratio of CaO, Al_2O_3 and SiO_2 is 1:1:2 approximately, which meets the stoichiometric proportion of anorthite. For the glass preparation, the starting materials potassium feldspar, CaO and Al_2O_3 were mixed together properly. The carefully mixed batch components were melted in an alumina crucible at 1500 °C for 6 h to form homogeneous melts. Glasses in frit form were obtained by quenching of the melts in cold water. The glass powders with different particle sizes (fine particle: 4.5 μm, coarse particle: 18.4 μm) were prepared by the wet ball-milling technique.

2.2. Glass-ceramic preparation

The aforementioned glass powders were mixed with 5 wt% polyvinyl alcohol solution as a binder, and then uniaxially pressed into discs with 40 mm in diameter under a 30 MPa pressure. The green discs were heated at 600 °C for 30 min to eliminate the binder and finally sintered in temperature range 850–1200 °C for 60 min. The heating rate for the sintering was maintained at 10 °C/min. After sintering, the samples were cooled to room temperature in the furnace. In order to explore the evolution process of crystalline phases, the glass powder discs were sintered at 850 °C, 900 °C, 950 °C and 1000 °C for different durations of 0 min, 10 min, 30 min, 60 min and 180 min with a heating rate of 10 °C/min.

2.3. DSC analysis

Glass powders were characterized by differential scanning calorimetry (DSC) using NETZSCH STA 449F3 (NETZSCH, Germany) with matched pairs of platinum–rhodium alloy crucibles. Alumina was used as the reference material. DSC measurements were performed at heating rates of 5 °C/min, 10 °C/min, 20 °C/min, and 30 °C/min within the temperature range 30–1200 °C to evaluate the glass crystallization activation energy (E_α) and the Avrami parameter (n). The tendency of the glasses to undergo bulk nucleation was assessed by performing DSC runs (10 °C/min) using glass powders with an average particle size of 4.5 μm and 18.4 μm.

2.4. XRD analysis

The glass-ceramics were pulverized into powder in an agate mortar for XRD analysis. The crystalline phases of the glass-ceramic samples were analyzed by the X-ray diffractometer (XRD, D8-FOCUS, Bruker, Germany) using copper K_α radiation, at 40 KV and 40 mA, with $2\theta = 5°$–$70°$ and $0.01° \ s^{-1}$.

2.5. SEM analysis

The microstructures of the etched surface and the fracture surface of the glass-ceramics were evaluated by a Field Emission Scanning Electron Microscope (FESEM, SU8010, Hitachi, Japan).

Table 1
Chemical composition of potassium feldspar and selected glass.

	SiO_2	Al_2O_3	CaO	K_2O	Na_2O	Fe_2O_3	MgO	SrO	TiO_2	BaO	others
Potassium feldspar composition in wt%	65.10	17.20	0.90	12.15	1.69	0.40	0.03	0.70	0.03	0.29	1.51
Selected glass composition in wt%	38.67	32.85	18.50	7.22	1.00	0.24	0.02	0.42	0.02	0.17	0.90
Selected glass composition in mol%	46.11	23.07	23.63	5.49	1.16	0.11	0.04	0.29	0.02	0.08	—

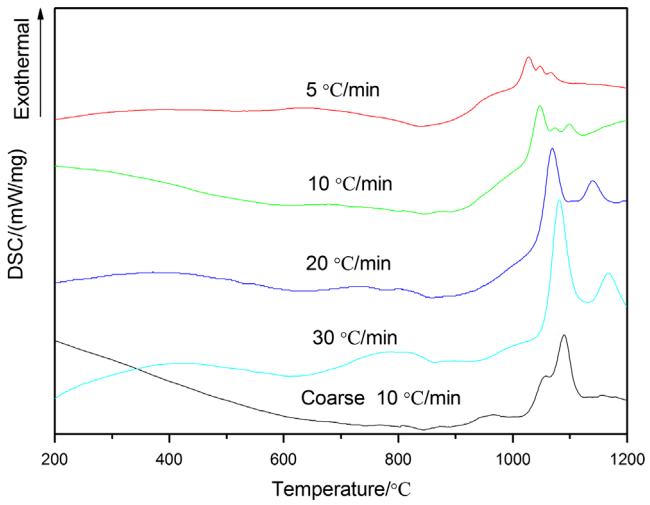

Fig. 1. DSC curves of fine glass powder at different heating rates and of coarse glass powder (bottom).

2.6. Properties evaluation

The bulk densities of sintered specimens were calculated through the Archimedes technique. Flexural strength of specimens ($30 \times 5 \times 2$ mm^3) was measured using a three-point bending method at the cross-head speed of 4 N/s. Coefficients of thermal expansion (CTEs) of samples (about $25 \times 6 \times 2$ mm^3) were measured using a dilatometer (NETZSCH DIL 402C, NETZSCH, Germany).

3. Results and discussion

Fig. 1 shows DSC curves of the fine glass powder at different heating rates and of the coarse glass powder (bottom). Comparing the DSC curves of coarse and of fine glass powder at a heating rate of 10 °C/min, it can be seen that even though there is a little difference on the outline of the crystallization exothermal peaks, peak temperatures are almost identical in temperature range 1000–1100 °C which gives a evidence that the crystallization mechanism for crystalline phases produced from the parent glass is bulk nucleation domination [14,31]. According to the DSC curves of the fine glass powder at different heating rates (5 °C/min, 10 °C/min, 20 °C/min, and 30 °C/min), the thermal parameters are summarized in Table 2. The DSC curves show two main glass transition temperatures (T_g) at about 600 °C and 800 °C, and glass crystallization temperatures (T_p) are in the range 1000–1100 °C. The DSC curves of the glass at low heating rates (5 °C/min and 10 °C/min) exhibit three exothermal peaks (T_{p1}, T_{p2} and T_{p3}). The second exothermal peak T_{p2} is gradually reduced and disappeared at heating rates of 20 °C/min and 30 °C/min. In contrast, the T_{p1} and T_{p3} are enhanced with the increase of heating rate. The T_g, T_{p1} and T_{p3} shift to high temperatures as the heating rate increases, showing the effect of thermal lag.

Fig. 2 shows XRD patterns of the glass-ceramics sintered at different temperatures. Two phases, anorthite ($CaAl_2Si_2O_8$) and kalsilite ($KAlSiO_4$), can be identified for the sample sintered at 900 °C. Besides the anorthite, leucite ($KAlSi_2O_6$) with a tetragonal structure and corundum (Al_2O_3) were formed in the samples sintered at 950 °C and above. The degree of crystallization of specimen sintered at 900 °C is higher than that of other specimens. And increasing sintering temperature strengthens the intensity of diffraction peaks of leucite.

Table 2
Thermal parameters of glass powder of a fine particle size.

α (°C/min)	T_{g1} (°C)	T_{g2} (°C)	T_{p1} (°C)	T_{p2} (°C)	T_{p3} (°C)
5	582.00	791.30	1027.51	1047.39	1067.57
10	594.11	811.37	1047	1072.58	1098.71
20	599.75	813.36	1069.21	—	1139.90
30	606.64	825.48	1081	—	1165.92

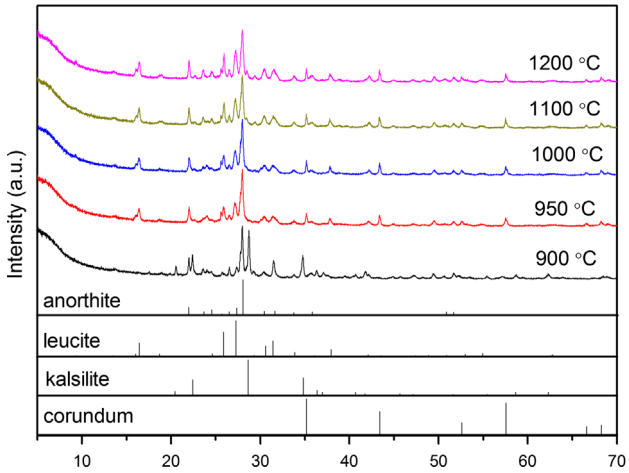

Fig. 2. XRD patterns of the glass-ceramics sintered at different temperatures.

In order to understand the evolution of crystalline phases of the glass-ceramics, the XRD patterns of the samples sintered at 850 °C, 900 °C, 950 °C and 1000 °C for different durations (0–180 min) are recorded and shown in Fig. 3.

The XRD analysis results show that the glass compact sintered at 850 °C for 180 min remains amorphous. When the sintering temperature was aroused to 900 °C and above, the crystallization took place. Fig. 3(a) shows the XRD patterns of glass-ceramics sintered at 900 °C. A typical amorphous pattern was recorded for the sample sintered at 900 °C for 0 min. Prolonging the holding time to 10 min, a few weak peaks emerged. And typical crystalline diffraction peaks inherent to anorthite and kalsilite appeared for the samples sintered at 900 °C for 30 min, 60 min and 180 min. As the sintering temperature increases, the crystal phases will be formed in a short time. Kalsilite and anorthite phases were formed in the glass-ceramics sintered at 950 °C for 10 min and 30 min, as shown in Fig. 3(b). Besides of the formation of anorthite, kalsilite would transform to leucite phase and corundum was formed simultaneity when the holding time was extended to 60 min and above. The reaction equation is expressed as following:

$$KAlSiO_4 + SiO_2(\text{amorphous}) \rightarrow KAlSi_2O_6 \quad (1)$$

The phase transition from kalsilite to leucite also happened when the glass compacts were sintered at 1000 °C for over 30 min, as shown in Fig. 3(c). According to the findings of Liu

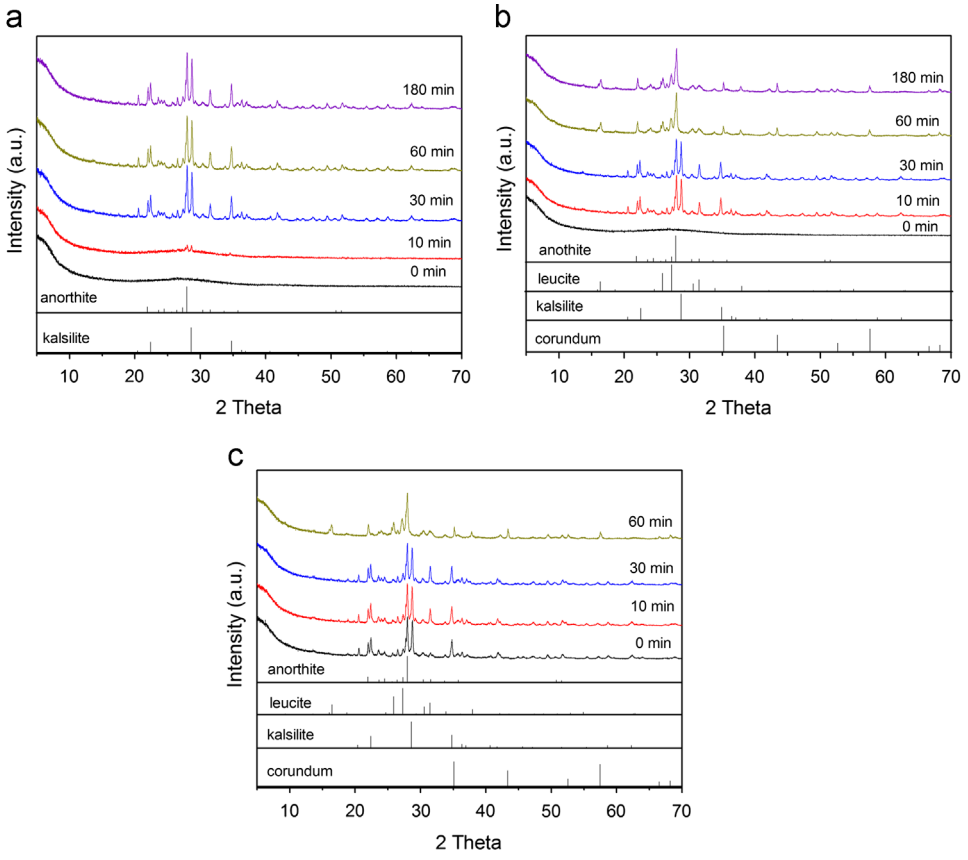

Fig. 3. XRD patterns of glass-ceramics sintered at different temperatures: (a) 900 °C, (b) 950 °C and (c) 1000 °C for different durations.

et al. [32] and Erbe et al. [33], kalsilite is metastable during the leucite crystallization process, which can be converted into leucite by wet chemical method or high temperature melting and crystallization method. So it can be derived that kalsilite phase is firstly formed in the samples sintered at and above 950 °C, and then transformed into leucite phase through reacting with SiO_2 in the glass phase.

The relationship between the fraction crystallization and the nucleation and growth rates is described by the Johnson–Mehl–Avrami (JMA) transformation kinetics [34]

$$-ln\alpha(1-x) = kt^n \tag{2}$$

where x is the fraction crystallized at a given temperature in time t; n is the Avrami exponent which is a dimensionless constant related to the nucleation and growth mechanisms; k is the reaction rate constant, which is related to the activation energy E.

In non-isothermal transformation studies, the crystallization exothermic peaks (T_p) on DSC traces of glasses were affected by the heating rate (α). When the heating rate (α) was slow, the crystalline phases have sufficient time to grow. Therefore, the T_p is low, and the crystallization exothermal peaks are flat. On the contrary, when the heating rate is fast, the crystallization lags and the T_p increases, and the crystallization exothermal peaks are sharp. According to the above exothermic crystallization characteristics and JMA equation, Kissinger proposed that the activation energy of a first order process can be determined from the variation in exothermal crystallization peaks with different heating rates of DSC by the following relationship [35]:

$$ln\frac{\alpha}{T_p^2} = -\frac{E}{RT_p} + C_1 \tag{3}$$

where C_1 is a constant, α is the heating rate in the DSC, E is the crystallization activation energy, T_p is the absolute temperature of the peak in DSC curves. The value of n can be attained from the following equation [36–38]:

$$ln(\Delta T) = -\frac{nE}{RT_i} + C_2 \tag{4}$$

here T_i is the random temperature in the DTA curves, T is the vertical displacement from the baseline to the line of the crystallization exothermic peak at the temperature T_i.

The value of the activation energy (E_α) can be calculated from the first exothermal peak temperature (T_{p1}) using the Kissinger method (Eq. (4)). Plot of $ln(\alpha/T_P^2)$ versus $1000/T_p$ is shown in Fig. 4 and the activation energy (E_α) calculated from the slope of the plot is 463.81 KJ/mol. For the determination of the crystallization mechanism, the crystallization kinetic parameters n and m are calculated. The value of m can be deduced from $n=m+1$ [39,40]. The values of n and m for different crystallization mechanisms have been summarized in References [10–13]. The values of n can be obtained from the slope of ln $\triangle T$ versus $1000/T$ plots, as shown in Fig. 5. The values of n at heating rates of 5 °C/min, 10 °C/min, 20 °C/min and 30 °C/min are 4.20, 3.66, 3.44 and 3.67, respectively.

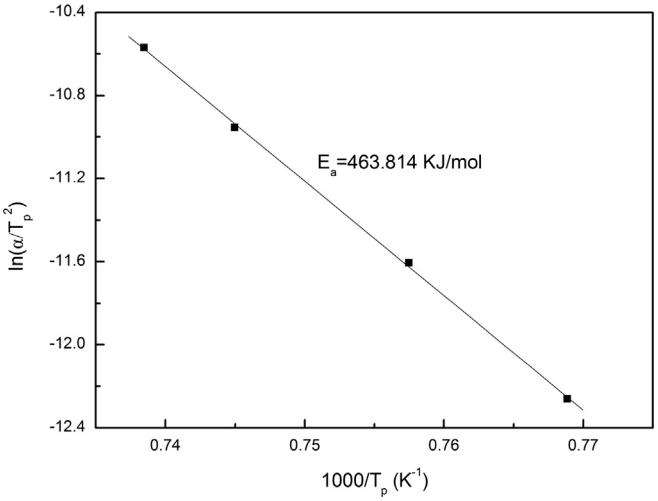

Fig. 4. Plot of $ln(\alpha/T_P^2)$ versus $1000/T_p$.

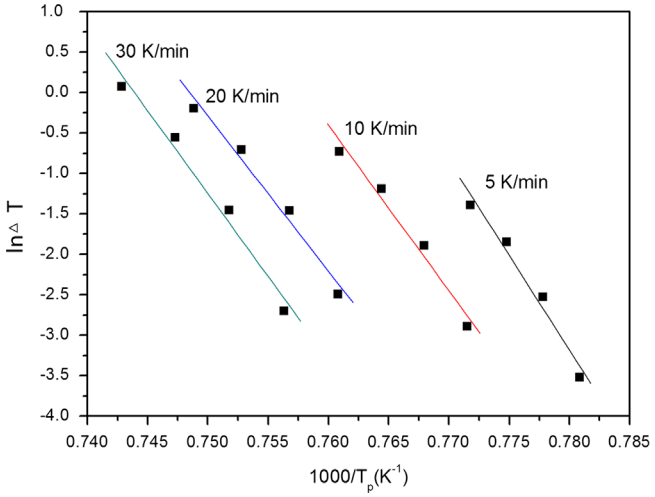

Fig. 5. Plots of ln $\triangle T$ versus $1000/T$ at different heating rates.

The mean value of n is 3.74 and that of m is 2.74. The mean value of n is close to 4 and the value of m is close to 3, which demonstrates the dominance of bulk nucleation and three-dimensional crystal growth mechanisms in the temperature range 1000–1100 °C.

Fig. 6 shows the SEM images of etched and fractured surfaces of the glass-ceramics sintered at different temperatures. It can be seen in Fig. 6(a) that column crystals accompanied with some granular grains were precipitated in the sample sintered at 900 °C for 60 min. Increasing sintering temperature enhanced the formation of granular grains, as shown in the Fig. 6 (b) (sintered at 950 °C for 60 min). In the samples sintered at 1000 °C and 1100 °C for 60 min, the column crystals disappeared and only granular grains were shown in Fig. 6(c and d). The granular grains are well uniformed with a mean diameter of about 300 nm, which is a benefit for the high strength of the glass-ceramics. In addition, it can be concluded that three-dimensional crystal growth mechanism happened in the temperature range 1000–1100 °C based on the fact that only three-dimensional granular grains were formed. But one-dimensional crystal growth mechanism happened in the temperature range 900–950 °C, which could be concluded from the column crystals. As seen in Fig. 6(e–h), the glass-ceramic fabricated at 900 °C has a loose structure and the glass-ceramics get denser with few pores at higher sintering temperatures. However, the number of pores increases for samples sintered at 1100 °C compared to that of samples sintered at 950 °C and 1000 °C. Therefore, the sintering temperature is a critical factor influencing the microstructure and even the crystallization mechanism of glass-ceramics.

The mechanical properties and thermal expansion characterization of glass-ceramics are dramatically affected by their compositions and microstructures, including the type and the content of crystalline phases and porosity, etc. [41–47]. Fig. 7 shows thermal expansion behavior of samples sintered within the temperature range of 900–1200 °C. The average coefficients of thermal expansion deduced from its slope are $5.69 \times 10^{-6}\,K^{-1}$, $10.85 \times 10^{-6}\,K^{-1}$, $11.03 \times 10^{-6}\,K^{-1}$ and $11.94 \times 10^{-6}\,K^{-1}$. Combining the results of XRD, the CTEs of samples containing leucite are about two times larger than those containing kalsilite. The high CTEs of samples containing leucite should be ascribed to the high CTE of the tetragonal leucite phase, and the loose microstructure of sample containing kalsilite (Fig. 6e) was demonstrated the main cause for the low CTE of the sample sintered at 900 °C. Additionally, the reason why the CTEs of glass-ceramics containing leucite slightly increased with sintering temperature can be ascribed to the increasing leucite.

Fig. 8 shows the variations of density and flexural strength of glass-ceramics with the sintering temperature. It can be seen that the glass-ceramics with high densities and high flexural strength can be obtained by sintering at 950 °C and above. The density values are in the range 2.4–2.6 g/cm^3, increasing sharply when the sintering temperature changes from 900 °C to 950 °C. The densities of the anorthite, leucite and kalsilite are 2.758 [48], 2.47 [49] and 2.619 [50] respectively. Even though the degree of crystallization of the sample sintered at 900 °C is higher than other samples and the density of kalsilite is also higher than that of leucite, the density of glass-ceramic sintered at 900 °C still the lowest because of the high level of porosity of the sample. On the one hand, the glass-ceramic was poorly sintered at 900 °C; on the other hand, the secondary porosity often appears due to the crystallization of phases of higher densities than the parent glass [51] of the same chemical composition as the crystalline phase. The calculated density of parent glass according to the Appen's [52] method of the same chemical composition as the kalsilite is 2.55 g/cm^3. If crystallization proceeds beyond a certain limit, then the occurrence of volume changes results in the development of new pores (defined as secondary porosity) and the enlargement of the existing ones [53]. The slight decrease of the density in the temperature range 950–1100 °C is due to the high porosity in samples caused by high crystallization rate at the high temperature, which can be demonstrated based on the fact that the number of pore in specimen sintered at sintered at 1100 °C is more than that of samples sintered at 950 °C and 1000 °C.

The flexural strength values are in the range 95–250 MPa, which are greatly higher than the previously reported anorthite glass-ceramics [15] and increase with the increase of sintering temperature and holding time. The flexural strength of sample

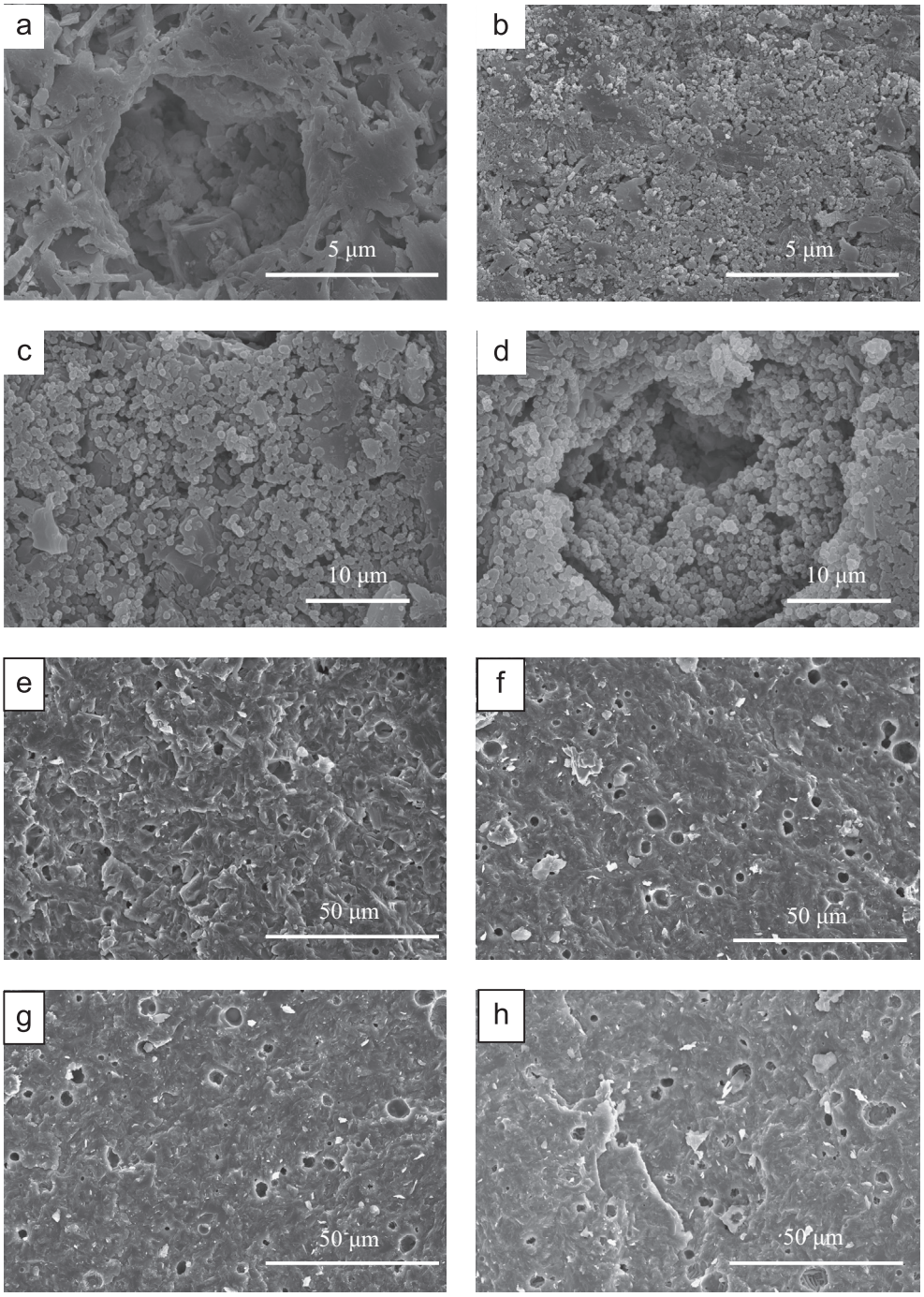

Fig. 6. SEM images of etched (a–d) and fractured (e–h) surfaces of the glass-ceramics sintered at 900 °C (a, e), 950 °C (b, f), 1000 °C (c, g) and 1100 °C (d, h).

sintered at 900 °C is the lowest because of the loose microstructure. When the sintering temperature is at and above 950 °C, the flexural strength of the glass-ceramics is obviously improved. And it enhanced even though the porosity of specimen sintered at 1100 °C is higher than that of specimens sintered at 950 and 1000 °C. Besides of the denser microstructure comparing to the specimen sintered at 900 °C, the formation of leucite is another key point to the high flexural strength of the glass-ceramics sintered at and above 950 °C. The transformation of leucite from high temperature cubic phase to the low temperature tetragonal phase will leads to a reversible 1.2% volume contraction. Together with the difference in thermal expansion between the tetragonal leucite crystals and the surrounding phases, high tangential compressive stresses around the leucite grains would be developed and maintained in the glass-ceramics during the cooling process, which are considered responsible for strengthening in glass-ceramics containing leucite [24–26].

4. Conclusions

The anorthite–leucite glass-ceramics were prepared by controlled crystallization of K_2O–CaO–Al_2O_3–SiO_2 quaternary

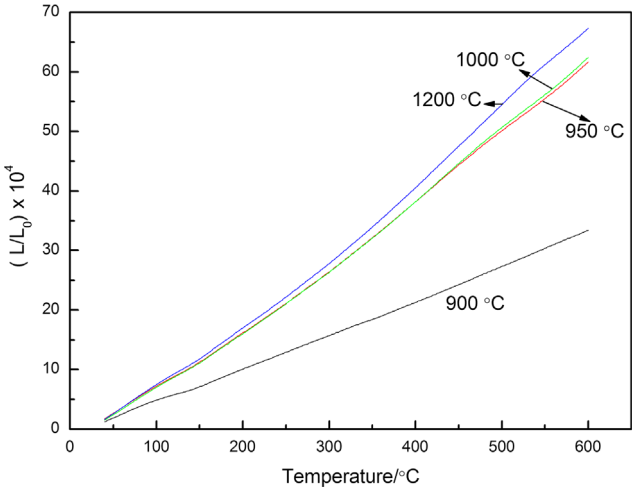

Fig. 7. Thermal expansion behavior of samples sintered within the temperature range of 900–1200 °C.

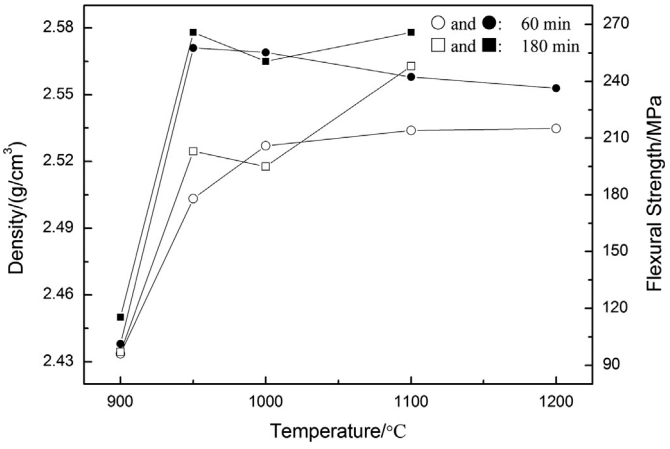

Fig. 8. Variations of density (● and ■) and flexural strength (○ and □) of glass-ceramics with the sintering temperature.

glass using potassium feldspar as a raw material. The formation mechanism of crystals in the glass-ceramics is bulk nucleation with three-dimensional crystal growth in the temperature range 1000–1100 °C. The crystalline phases and microstructures of the glass-ceramics are obviously affected by the sintering process. For the anorthite–leucite glass-ceramics, kalsilite emerged firstly and reacted with SiO_2 in the glass phase to form leucite. The glass-ceramics with high flexural strength and high CTEs were obtained by sintering at and above 950 °C. The high flexural strength and high CTEs are attributed to the formation of leucite.

Acknowledgments

The work was financial supported by the National Science and Technology Support Plan of Peoples Republic of China (No. 2011BAB03B01).

References

[1] P.W. McMillan, Glass-Ceramics, Academic Press, New York, 1979.
[2] A.M. Hu, M. Li, D. Mao, Controlled crystallization of glass-ceramics with two nucleating agents, Materials Characterization 60 (2009) 1529–1533.
[3] W. Hölland, G. Beall, Glass-Ceramic Technology, The American Ceramic Society, Ohio, 2002.
[4] L.A. Zhunina, V.N. Shara, V.F. Tsitko, N.N. Khrikova, The Structure of Glass, Consultant Bureau, New York, 1964.
[5] M. Kang, S. Kang, Effects of Al_2O_3 addition on physical properties of diopside based glass-ceramics for LED packages, Ceramics International 38 (2012) S551–S555.
[6] L. Yu, H. Xiao, Y. Cheng, Influence of magnesia on the structure and properties of MgO–Al_2O_3–SiO_2–F glass-ceramics, Ceramics International 34 (2008) 63–68.
[7] J. Banjuraizah, H. Mohamad, Z.A. Ahmad, Synthesis and characterization of xMgO–1.5Al_2O_3–5SiO_2 (x=2.6–3.0) system using mainly talc and kaolin through the glass route, Materials Chemistry and Physics 129 (2011) 910–918.
[8] A.X. Lu, Z.B. Ke, Z.H. Xiao, X.F. Zhang, X.Y. Li, Effect of heat-treatment condition on crystallization behavior and thermal expansion coefficient of Li_2O–ZnO–Al_2O_3–SiO_2–P_2O_5 glass-ceramics, Journal of Non-Crystalline Solids 353 (2007) 2692–2697.
[9] P. Goharian, A. Nemati, M. Shabanian, A. Afshar, Properties, crystallization mechanism and microstructure of lithium disilicate glass-ceramic, Journal of Non-Crystalline Solids 356 (2010) 208–214.
[10] M.M. Kržmanc, U. Došler, D. Suvorov, L. Pinckney, Effect of a TiO_2 nucleating agent on the nucleation and crystallization behavior of MgO–B_2O_3–SiO_2 glass, Journal of the American Ceramic Society 95 (2012) 1920–1926.
[11] P.K. Maiti, A. Mallik, A. Basumajumdar, P. Guha, Influence of barium oxide on the crystallization, microstructure and mechanical properties of potassium fluorophlogopite glass-ceramics, Ceramics International 38 (2012) 251–258.
[12] S. Jang, S. Kang, Influence of MgO/CaO ratio on the properties of MgO–CaO–Al_2O_3–SiO_2 glass-ceramics for LED packages, Ceramics International 38 (2012) S543–S546.
[13] M. Romero, J. Martín-Márquez, J.M. Rincón, Kinetic of mullite formation from a porcelain stoneware body for tiles production, Journal of the European Ceramic Society 26 (2006) 1647–1652.
[14] C.L. Lo, J.G. Duh, B.S. Chiou, Low temperature sintering and crystallisation behaviour of low loss anorthite-based glass-ceramics, Journal of Materials Science 38 (2003) 693–698.
[15] V.M.F. Marques, D.U. Tulyaganov, S. Agathopoulos, V.K. Gataullin, G. P. Kothiyal, J.M.F. Ferreira, Low temperature synthesis of anorthite based glass-ceramics via sintering and crystallization of glass-powder compacts, Journal of the European Ceramic Society 26 (2006) 2503–2510.
[16] C.L. Lo, J.G. Duh, B.S. Chiou, W.H. Lee, Low-temperature sintering and microwave dielectric properties of anorthite-based glass-ceramics, Journal of the American Ceramic Society 85 (2002) 2230–2235.
[17] C.L. Lo, J.G. Duh, B.S. Chiou, W.H. Lee, Microstructure characteristics for anorthite composite glass with nucleating agents of TiO_2 under non-isothermal crystallization, Materials Research Bulletin 37 (2002) 1949–1960.
[18] C.J. Dileep Kumar, E.K. Sunny, N. Raghu, N. Venkataramani, A. R. Kulkarni, Synthesis and characterization of crystallizable anorthite-based glass for a low-temperature cofired ceramic application, Journal of the American Ceramic Society 91 (2008) 652–655.
[19] C.J. Jeon, J.K. Lee, E.S. Kim, Effect of Al_2O_3 on thermal properties of 0.5$CaAl_2Si_2O_8$–0.5$CaMgSi_2O_6$ glass-ceramics, Ceramics International 38 (2012) 557–561.
[20] D. Momete, C.V. Brovarone, O. Bretcanu, E. Verne, Preparation and investigation of a glass in the system Al_2O_3–SiO_2–CaO for dental applications, Materials Letters 60 (2006) 3045–3047.
[21] C. Siligardi, P. Miselli, L. Lusvarghi, M. Reginelli, Influence of CaO–ZrO_2–Al_2O_3–SiO_2 glass-ceramic frits on the technological properties of porcelain stoneware bodies, Ceramics International 37 (2011) 1851–1858.
[22] R. Dimitrijevic, V. Ddondur, Synthesis and characterization of $KAlSiO_4$ polymorphs on the SiO_2–$KAlO_2$ join, Journal of Solid State Chemistry 115 (1995) 214–224.

[23] D.C. Palmer, E.K.H. Salje, W.W. Schmal, Phase transitions in leucite: X-ray diffraction studies, Physics and Chemistry of Minerals 16 (1989) 714–719.
[24] M.J. Cattell, T.C. Chadwick, J.C. Knowles, R.L. Clarke, The crystallization of an aluminosilicate glass in the K_2O–Al_2O_3–SiO_2 system, Dental Materials 21 (2005) 811–822.
[25] I.L. Denry, J.J.R. Mackert, J.A. Holloway, S.F. Rosenstiel, Effect of cubic leucite stabilisation on the flexural strength of feldspathic dental porcelain, Journal of Dental Research 75 (1996) 1928–1935.
[26] P. Wange, T. Höche, C. Rüssel, J.D. Schnapp, Microstructure-property relationship in high-strength MgO–Al_2O_3–SiO_2–TiO_2 glass-ceramics, Journal of Non-Crystalline Solids 298 (2002) 137–145.
[27] P.P. Kist, I.L. Aurelio, K.A. Fukushima, L.G. May, Bur grit: effect on the flexural strength of leucite-reinforced glass-ceramic, Dental Materials 28 (2012) 28–29.
[28] X. Chen, T.C. Chadwick, R.M. Wilson, R.G. Hill, M.J. Cattell, Crystallization and flexural strength optimization of fine-grained leucite glass-ceramics for dentistry, Dental Materials 27 (2011) 1153–1161.
[29] M.J. Cattell, T.C. Chadwick, J.C. Knowles, E. Lynch, Flexural strength optimisation of a leucite reinforced glass ceramic, Dental Materials 17 (2001) 21–33.
[30] M.D. Fonseca, F.T. Silva, T. Ogasawara, Study of the crystallization of leucite in feldspar glass matrix, Journal of Thermal Analysis and Calorimetry 106 (2011) 343–346.
[31] V.K. Marghussian, O.U. Balazadegan, B. Eftekhari-yekta, Crystallization behaviour, microstructure and mechanical properties of cordierite–mullite glass ceramics, Journal of Alloys and Compounds 484 (2009) 902–906.
[32] C.L. Liu, S. Komarneni, R. Roy, Seeding effects on crystallization of $KAlSi_3O_8$, $RbAlSi_3O_8$, and $CsAlSi_3O_8$ gels and glasses, Journal of the American Ceramic Society 77 (1994) 3105–3112.
[33] E.M. Erbe, R.S. Sapieszko, Chemically Derived Leucite, US Patent 5622551, 1997.
[34] W.A. Johnson, R.F. Mehl, Reaction kinetics in processes of nucleation and growth, Transaction of American Institute of Mining, Metallurgical, and Petroleum Engineers 135 (1939) 416–442.
[35] I.W. Donald, Crystallization kinetics of a lithium zinc silicate glass studied by DTA and DSC, Journal of Non-Crystalline Solids 345–346 (2004) 120–126.
[36] H. Shao, K. Liang, F. Peng, Crystallization kinetics of MgO–Al_2O_3–SiO_2 glass-ceramics, Ceramics International 30 (2004) 927–930.
[37] G.O. Piloyan, I.D. Ryabchikov, O.S. Novikova, Determination of activation energy of chemical reactions by differential thermal analysis, Nature 212 (1966) 1229.
[38] M. Avrami, Kinetics of phase change. I general theory, Journal of Chemical Physics 7 (1939) 1103–1113.
[39] R. Iordanova, E. Lefterova, I. Uzunov, D. Klissurshi, Non-isothermal crystallization kinetics of V_2O_5–MoO_3–Bi_2O_3 glasses, Journal of Thermal Analysis and Calorimetry 70 (2002) 393–404.
[40] Y. Cheng, H. Xiao, W. Guo, W. Guo, Structure and crystallization kinetics of Bi_2O_3–B_2O_3 glasses, Thermochimica Acta 444 (2006) 173–178.
[41] M. Mirsaneh, I.M. Reaney, P.F. James, P.V. Hatton, Effect of CaF_2 and CaO substituted for MgO on the phase evolution and mechanical properties of K-fluorrichterite glass ceramics, Journal of the American Ceramic Society 89 (2006) 587–595.
[42] K. Lin, W. Zhai, S.Y. Ni, J. Chang, Y. Zeng, W.J. Qian, Study of the mechanical property and in vitro biocompatibility of $CaSiO_3$ ceramics, Ceramics International 31 (2005) 323–326.
[43] S.-F. Wang, Y.-R. Wang, Y.-F. Hsu, C.-C. Chuang, Effect of additives on the thermal properties and sealing characteristic of BaO–Al_2O_3–B_2O_3–SiO_2 glass-ceramic for solid oxide fuel cell application, International Journal of Hydrogen Energy 34 (2009) 8235–8244.
[44] G.A. Khater, M.H. Idris, Expansion characteristics of some Li_2O–BaO–Al_2O_3–SiO_2 glasses and glass-ceramics, Ceramics International 32 (2006) 833–838.
[45] G.H. Beall, Refractory glass-ceramics based on alkaline earth aluminosilicates, Journal of the European Ceramic Society 29 (2009) 1211–1219.
[46] V. Cannillo, F. Pierli, S. Sampath, C. Siligardi, Thermal and physical characterisation of apatite/wollastonite bioactive glass-ceramics, Journal of the European Ceramic Society 29 (2009) 611–619.
[47] T. Zhang, Q. Zou, Tuning the thermal properties of borosilicate glass ceramic seals for solid oxide fuel cells, Journal of the European Ceramic Society 32 (2012) 4009–4013.
[48] JCPDS Card of Anorthite-Annealed no. 89-1472.
[49] JCPDS Card of Leucite no. 71-1147.
[50] JCPDS Card of Kalsilite no. 85-1413.
[51] D.U. Tulyaganov, S. Agathopoulos, H.R. Fernandes, J.M.F. Ferreira, Processing of glass-ceramics in the SiO_2–Al_2O_3–B_2O_3–MgO–CaO–Na_2O–(P_2O_5)–F system via sintering and crystallization of glass powder compacts, Ceramics International 32 (2006) 195–200.
[52] A.A. Appen, The Chemistry of Glasses, Himiq, Leningrad, Russian, 1975.
[53] C. Lira, A.P.N. Oliveira, O.E. Alarcon, Sintering and crystallization of CaO–Al_2O_3–SiO_2 glass powder compacts, Journal of Glass Science and Technology Part A 42 (2001) 91–96.